

# ATMOSPHERIC TEMPERATURE PROFILE MEASUREMENTS USING MOBILE HIGH SPECTRAL RESOLUTION LIDAR

Ilya I. Razenkov, Edwin W. Eloranta

*University of Wisconsin, 1225 W. Dayton St., Madison, WI, 53706, USA, razenkov@wisc.edu*

## ABSTRACT

The High Spectral Resolution Lidar (HSRL) designed at the University of Wisconsin-Madison discriminates between Mie and Rayleigh backscattering [1]. It exploits the Doppler effect caused by thermal motion of molecules, which broadens the spectrum of the transmitted laser light. That allows for absolute calibration of the lidar and measurements of the aerosol volume backscatter coefficient. Two iodine absorption filters with different absorption line widths (a regular iodine vapor filter and Argon buffered iodine filter) allow for atmospheric temperature profile measurements. The sensitivity of the measured signal-to-air temperature ratio is around 0.14%/K. The instrument uses a shared telescope transmitter-receiver design and operates in eye-safe mode (the product of laser average power and telescope aperture equals  $0.1 \text{ Wm}^2$  at 532 nm).

## 1. INTRODUCTION

The atmospheric temperature is an important parameter that describes the atmospheric state. It plays an important role in many atmospheric processes. Passive remote sensors lack the spatial resolution necessary for many applications. Radiosonde measurements are usually available only twice a day. Some types of lidars are capable of measuring the atmospheric temperature profile with a relatively large spatial resolution and with more frequent measurement.

Several investigators have made atmospheric temperature profile measurements using a High Spectral Resolution Lidar (HSRL) [2-5]. These techniques suffer from low signal-to-noise ratio, low sensitivity to air temperature, and/or operate highly exceeding the eye-safe limit on the transmitted laser power; and also suffer from limitations in filter and laser frequency stability.

The standard HSRL technique requires the atmospheric temperature and pressure profile for instrument calibration. In this paper, we report the atmospheric temperature profile measurements performed by the University of Wisconsin –

Madison High Spectral Resolution Lidar. Two iodine absorption filters with different absorption line widths enable atmospheric temperature profile measurements. A molecular iodine I<sub>2</sub> vapor filter provides standard HSRL measurements. A second channel using an argon buffered iodine filter provides additional information for atmospheric temperature measurements. The instrument's capability to measure the atmospheric temperature profile makes it intrinsically calibrated. The presented temperature measurement technique requires a superior instrument performance in order to achieve good measurement accuracy. Work done in attempt to perfect this technique have improved instrument performance and data quality for standard HSRL measurements.

## 2. HIGH SPECTRAL RESOLUTION LIDAR SYSTEM

The simplified schematic of the HSRL lidar is shown in Figure 1. The transmitter uses an injection seeded diode pumped Nd:YAG laser. The laser operates at 4kHz repetition rate. The single mode diode DFB seed laser (1064 nm) is used to injection seed the host laser cavity. The seed laser is frequency locked to the center of iodine absorption line #1109 using a frequency locking setup with active control loop. The setup uses a 100mm long iodine absorption cell and two energy monitors. The computer controlled DAQ applies voltage to the seed laser controller and does a slow frequency tuning of the laser. The laser cavity controller dithers the host cavity end mirror changing the output frequency with around 12MHz amplitude and measures the absorption line slope at the frequency. The zero slope value corresponds to the bottom of the absorption line. The slope information is transferred to the computer providing an active feedback for laser frequency control. That provides the frequency locking accuracy of around 12MHz with a frequency jitter of around 12MHz amplitude. Some of the lidar transceiver properties are summarized in Table 1.

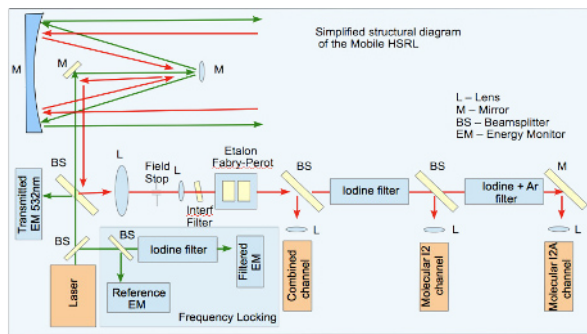


Figure 1. A simplified structural diagram of HSRL system.

**Table 1: Lidar parameters.**

Wavelength	532 nm
Transmitted eye-safe power	0.3W @532nm
Transmitter Spectral width	< 60 MHz
Spectral purity	>5000:1
Scanning telescope (Dall-Kirkham)	20x, Diam 400 mm
Receiver Spectral bandwidth	8 GHz
Iodine blocking filters' bandwidth	1.8 GHz (narrow filter), 2.85 GHz (wide filter)

Some portion of the laser light is picked off from the beam by a wedged beam pick-off for frequency locking setup, laser spectrum quality control and the interferometer. The broadband beam splitter (R/T=65/35S) is used as a transceiver switch. Then, the beam is further expanded by 20x Dall-Kirkham telescope (400 mm aperture) and transmitted into the atmosphere. The telescope is shared between transmitter and receiver. The sky background noise is rejected by the interference filter (0.35 nm FWHM) and Fabry-Perot etalon (FWHM=7.5 GHz, FSR=375 GHz, peak transmission is 76%).

An argon-broadened filter allows ~0.1% minimum transmission in the center of the 1109 line and cannot provide sufficient rejection of aerosol signal. For that reason a serial arrangement of the filters is used.

### 3. ARGON BUFFERED IODINE FILTER EXPERIMENTS

A buffer gas such as argon added to the filter can broaden the absorption line of the iodine filter. A series of experiments were performed in order to find the optimum pressure of the argon gas in the iodine cell. The filter is optimized to provide sensitivity to the atmospheric temperature and transmission of molecular signal. The

experimental setup for iodine absorption line broadening with argon buffer gas is shown in Figure 2. The filter transmission curves are shown in Figure 3.

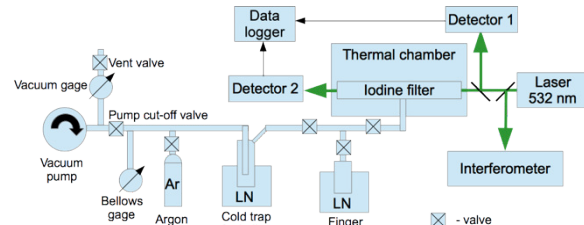


Figure 2. Experimental setup for iodine filter broadening using Argon gas.

The molecular iodine absorption spectrum changes as the argon pressure increases: the line width increases, peak absorption and continuum transmission decrease.

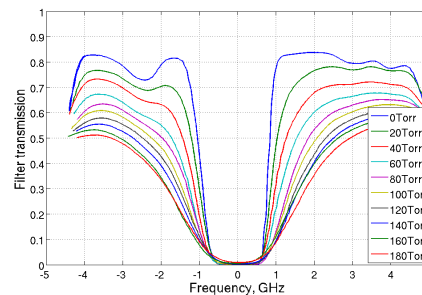


Figure 3. A set of experimentally measured molecular iodine filter transmission curves for different argon gas pressures ranging from 0 Torr to 180 Torr.

The absorption filters contain a fixed amount of iodine to provide stable filter properties. Heaters maintain all the iodine in the gaseous phase and ensure that no iodine condensation occurs on the windows of the cell.

### 4. CALCULATION OF OPTIMUM ARGON PRESSURE

The selection of the optimum pressure for the broadened iodine filter is done by modeling the lidar temperature measurements. The real lidar returns from the operating instrument are used to perform the analysis that accounts for the actual instrument efficiency. The ratio  $R$  of the signals of the two molecular channels is a function of the atmospheric temperature and pressure. The received signal in the channels *Molecular I2* ( $N_{m,1}$ ) and *Molecular I2A* ( $N_{m,2}$ ) are:

$$N_{m,1}(z) = N_0(z)(1 - T_{bs})f_{m,1}(z),$$

$$N_{m,2}(z) = N_0(z) T_{bs}f_{m,2}(z),$$

where  $f_{m,1}(z) = \int F_1(\nu)\mathcal{R}(T(z), P(z), \nu)d\nu$ ,

$f_{m,2}(z) = \int F_1(\nu)F_2(\nu)\mathcal{R}(T(z), P(z), \nu)d\nu$ ,

and  $\int \mathcal{R}(T(z), P(z), \nu)d\nu = 1$ ,  $N_0(z)$  – number of photons received from a distance  $z$  (actual lidar counts);  $T_{bs}$  – beamsplitter transmission;  $\nu$  – frequency;  $F_1(\nu), F_2(\nu)$  – transmission spectrums of a standard iodine and broadened iodine filters;  $\mathcal{R}(T, P, \nu)$  – spectrum of molecular return from Tenti's s6 model;  $T(z), P(z)$  – atmospheric temperature and pressure;  $T(z), P(z)$  are the temperature and pressure measured by radiosonde.

The ratio of the signals in two channels is the function of temperature and pressure for a given value of  $T_{bs}$ :

$$R(z) = \frac{N_{m,1}(z)}{N_{m,2}(z)} = \frac{1 - T_{bs} f_{m,1}(T(z), P(z))}{T_{bs} f_{m,2}(T(z), P(z))}$$

The instrument temperature sensitivity coefficient  $\frac{dR}{dT}$  at each altitude can be calculated by using the expression above.

The photon counting error is calculated by using the following relationship:

$$dR_{er} = \sqrt{\frac{N_{m,1}}{N_{m,2}^2} + \frac{N_{m,1}^2}{N_{m,2}^3}}.$$

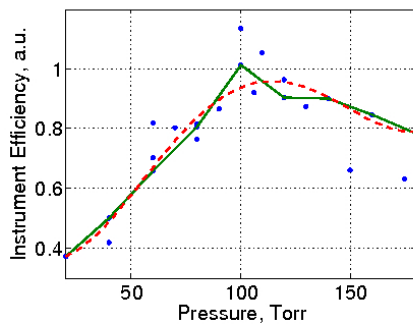


Figure 4. Modeled instrument temperature efficiency at 5 km as a function of argon pressure. Scattered blue dots are the efficiencies for different tests with various amount of iodine in the cell, the solid green line is for a test with a fixed amount of iodine and the dashed green line is the third order polynomial fit to all the tests.

The ratio of the sensitivity coefficient (signal-to-air temperature ratio) to the counting error (instrument T efficiency) is used to find the

optimum argon gas pressure for broadened filter. The curve for the instrument T efficiency as a function of buffer gas pressure calculated at 5 km is shown in Figure 4. The maximum of the ratio is found to be at around 110 Torr of the argon gas pressure. The instrument temperature sensitivity coefficient  $\frac{dR}{dT}$  for broadened filter (110 Torr) is around 0.14%/K.

## 5. ATMOSPHERIC TEMPERATURE MEASUREMENT RESULTS

The atmospheric temperature profile measurement requires the instrument calibration. The channels' transmission spectrum functions  $\xi_1(\nu)F_1(\nu)$ ,  $\xi_2(\nu)F_1(\nu)F_2(\nu)$  (where  $\xi_1, \xi_2$  are the channel gains) are measured by performing a laser frequency scans across the receiver bandwidth. This provides the filter spectral bandpass and the relative sensitivity of the channels.

To obtain the atmospheric temperature we assume that the pressure at a starting range height is known. Then the temperature follows from the ratio of the received photon counts of the two molecular channels. When the temperature and pressure at one altitude are know, the pressure at the next range bin can be obtained by using the relationships for hydrostatic balance and ideal gas law. By repeating this, the temperature and pressure profiles are obtained.

The atmospheric temperature profile measured on the March 11, 2015 from 800 to 1500 UTC Madison, WI is shown in the Figure 5. The vertical resolution is 300 meters. The temperature profile measured by the HSRL still exhibits an offset between -5 and +5 K when compared with the radiosonde sounding result. A correction on the relative gain of the two molecular channels must be applied for its correction. This correction factor is determined by matching the lidar temperature and balloon temperature at one range height.

The difference in optical alignment of the two channels introduces a range dependent differential geometry error in the temperature measurements. The iodine absorption filters in the instrument are mounted in the motorized mechanical mounts and can be remotely removed from the received signal beam path without disturbing the optics. The correction for the range dependent alignment error

is performed by measuring the profile of the ratio of the two molecular channels when the broadened absorption filter is removed from the optical path. This range dependent correction is applied to the relative gain of the two channels. The measured differential geometry correction profile and the temperature error associated with it are shown in the Figure 6.

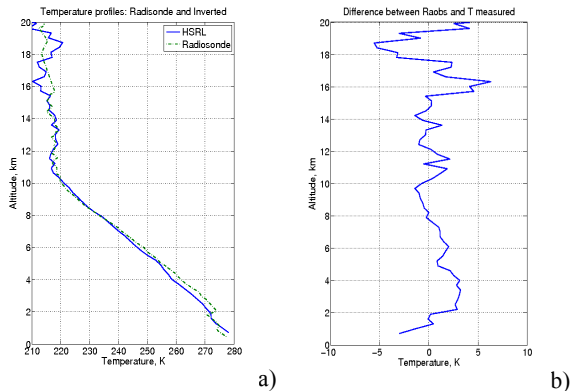


Figure 5. a) Measured atmospheric temperature profile (blue, solid) March 11, 2015 from 800 to 1500 UTC Madison, WI and radiosonde temperature profile (green, dashed) 12UTC Green Bay, WI sounding; b) The difference of lidar and radiosonde measured atmospheric temperature profiles.

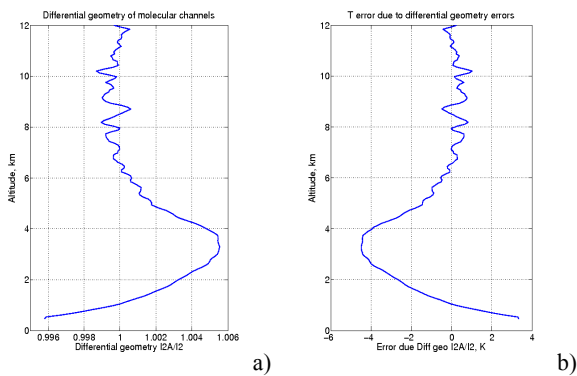


Figure 6. a) Measured differential geometry correction; b) Correction for differential geometry error.

The difference in geometry of the two channels is the largest source of errors. The inverted profile mismatches to the radiosonde observations in the lower 3 km. We assume that it is caused by the changes in the differential geometry and nonlinear detector response. The sensitivity of the instrument is relatively low, which requires a precise measurement (long averaging time), accurate correction of the channel relative overlaps (differential geometry), long term mechanical stability for optics, accurate

calibration and frequency locking, stability of detector gains and linearity of detector response.

## 6. CONCLUSIONS

We have reported the atmospheric temperature profile measurements performed by our HSRL lidar. This is made possible by using two iodine absorption filters with different absorption line widths. The instrument's signal-to-air temperature sensitivity is 0.14 %/K. The instrument has an advantage of moderate temperature sensitivity, relatively high efficiency, and eye-safe operation over previously reported works.

The temperature measurement accuracy currently lacks the long-term mechanical stability of optics, stability of detector gains and linearity of detector response. The instrument requires future improvement for robust routine measurements that will be useful for meteorological applications.

## ACKNOWLEDGEMENT

This work is supported by the Space Science and Engineering Center University of Wisconsin – Madison.

## REFERENCES

- [1] Eloranta, E. W.: High Spectral Resolution Lidar, in *Lidar: Range-Resolved Optical Remote Sensing of the Atmosphere*, Klaus Weitkamp ed., Springer, NY, pp. 25-30.
- [2] Shimizu H. et al, 1986: Atmospheric temperature measurement by a high spectral resolution lidar, *Applied Optics*, Vol. 25, Issue 9, pp. 1460-1466 (1986).
- [3] Dengxin H., 2004: Ultraviolet high-spectral resolution Rayleigh-Mie lidar with a dual-pass Fabry-Perot etalon for measuring atmospheric temperature profiles of the troposphere, *Applied Optics*, Vol. 44 Issue 7, pp.1305-1314 (2005).
- [4] Hair J.W. et al, 2001: “High spectral resolution lidar with iodine-vapor filters: measurement of atmospheric-state and aerosol profiles”, *Applied Optics*, Vol. 40, Issue 30, pp. 5280-5294 (2001).
- [5] Liu Z-S. et al 2009: Iodine-filter-based high spectral resolution lidar for atmospheric temperature measurements, *Optics Letters*, Vol. 34, Issue 18, pp. 2712-2714 (2009).